

SPARC: A Signal of Astrocytic Neoplastic Transformation and Reactive Response in Human Primary and Xenograft Gliomas

SANDRA A. REMPEL, PHD, WILLIAM A. GOLEMBIESKI, BS, SHUGANG GE, MD, NANCY LEMKE, HTL, KOST ELISEVICH, MD, PHD, TOM MIKKELSEN, MD, AND JORGE A. GUTIÉRREZ, MD

Abstract. In an attempt to identify genetic alterations occurring early in astrocytoma progression, we performed subtractive hybridization between astrocytoma and glioblastoma cDNA libraries. We identified secreted protein acidic and rich in cysteine (SPARC), a protein implicated in cell-matrix interactions, as a gene overexpressed early in progression. Northern blot and immunohistochemical analyses indicated that transcript and protein were both elevated in all tumor specimens (grades II–IV) examined when compared with levels in normal brain. The level of SPARC expression was found to be tumor-dependent rather than grade-related. Immunohistochemically, SPARC protein was found to be overexpressed in 1) cells in the less cellularly dense regions within the tumor mass, 2) histomorphologically neoplastic-looking cells in adjacent normal brain at the tumor/brain interface, 3) neovessel endothelial cells in both the tumor and adjacent normal brain, and 4) reactive astrocytes in normal brain adjacent to tumor. Using a combination of DNA *in situ* hybridization and protein immunohistochemical analyses of the human/rat xenograft, SPARC expression was observed in the human glioma cells within the tumor mass, and in cells that invaded along vascular basement membranes and individually into the rat brain parenchyma, suggesting it may be an invasion-related gene. While it remains to be determined whether SPARC functionally contributes to tumor cell invasion, these data suggest that the early onset of increased SPARC expression, though complex, may serve as a signal indicative of neoplastic astrocytic transformation and reactive response to tumor-induced stress.

Key Words: Astrocytomas; Gliomas; Neoplastic Transformation; Stress Response; SPARC; Xenograft.

INTRODUCTION

The poor prognosis of glioma patients is largely due to the highly infiltrative nature of these tumors and the inability to completely surgically resect or eradicate the infiltrating tumor cells by adjuvant therapies. The ability of a tumor cell to migrate into adjacent brain tissue is dependent upon the processes that govern cell migration, including the modulation of matrix degradation and cell-matrix and cell-cell interactions (1). Cell-matrix interactions are regulated, in part, by the balanced interplay between adhesive and counteradhesive proteins and an upset in the balance of their expression may favor increased cell migration.

Secreted protein acidic and rich in cysteine (SPARC) (2) is a member of the counteradhesive family of proteins (3). It is a developmentally regulated, secreted glycoprotein expressed in a number of fetal cell types, particularly during tissue remodeling and vascular morphogenesis (4), and can be highly expressed in response to stress (5). In the brain, SPARC is expressed in fetal astrocytes, in the tunica media and adventitia of developing vessels (4), and is restricted to astrocytes in synaptic rich regions in the adult brain (6). The brain extracellular matrix (ECM) is composed of laminin, fibronectin, vitronectin, collagens I, III, IV, and V, entactin, heparin sulfate, hyaluron,

and glycosaminoglycans (7). Of these constituents, SPARC interacts with collagens I, III, IV and V (3) and has been shown to bind directly to vitronectin (8), a multifunctional adhesive protein that is a component of brain vascular basement membranes.

SPARC secreted into the ECM is proposed to modulate cell adhesion by initiating a receptor-mediated signaling event (3). Downstream effects include changes in cytoplasmic components associated with focal adhesions (9), redistribution of vinculin from a punctate to diffuse localization (9), redistribution of F-actin to the cell periphery (9), and increased expression of collagenase, stromelysin, and the 92 kd gelatinase (10), enzymes that participate in the degradation of ECM matrices. Thus, SPARC's function in the modulation of cell-matrix interactions during fetal tissue development and vascular morphogenesis could also promote tumor cell migration if inappropriately expressed (reviewed in 3).

Increased SPARC expression has been observed in a number of malignant tumor types (11) including breast (12) and colon (13) and 2 low grade gliomas (11). Furthermore, melanoma cells transfected with an antisense SPARC construct and injected into the flanks of nude mice were unable to promote tumor formation *in vivo* (14). Thus, it appears that the inappropriate expression of SPARC may directly contribute to tumor pathogenesis.

In this study, we identified SPARC as a gene that is highly overexpressed in astrocytomas using subtractive hybridization, cloning and partial sequencing of the full-length cDNA. We further characterized its expression in human astrocytic tumors, grades II–IV, and in a human/rat xenograft model. In addition to expression in neoves-

From the Henry Ford Midwest Neuro-Oncology Center and the Departments of Neurosurgery (S.A.R., W.A.G., S.G., N.L., K.E., T.M.), Neurology (T.M.), and Pathology (J.A.G.), Henry Ford Health Sciences Center, Detroit, Michigan.

Correspondence to: Sandra A. Rempel, PhD, Department of Neurosurgery, Room 3096, Education and Research Building, Henry Ford Health Sciences Center, 2799 West Grand Blvd., Detroit MI 48202.

sel endothelial cells. SPARC was highly expressed in astrocytic tumors of all grades, in tumor cells invading adjacent brain, and in reactive astrocytes at the tumor/brain interface. These data suggest that SPARC is a candidate invasion-related gene overexpressed early in astrocytoma progression, and may serve as a signal indicative of astrocytic neoplastic transformation and reactive response to tumor-induced stress.

MATERIALS AND METHODS

cDNA Library Construction

Two cDNA libraries were constructed (15) for subtractive hybridization using RNA extracted from low grade astrocytomas and high grade glioblastomas multiforme (GBMs). RNA was pooled from several tumors of the same grade to eliminate possible patient-specific variations occurring in astrocytoma progression. RNA was extracted using the LiCl procedure of Auffray and Rugeon (16) from 4 astrocytoma tumor biopsy specimens (TM88, TM89, TM90, TM172). RNA was similarly extracted from 7 glioblastoma tumor biopsy specimens (TM12, TM162, TM169, TM173, TM177, TM182, TM185). Each pool of RNA was treated similarly as follows. RNA was separated from DNA by CsCl gradient centrifugation (17, 18) and used in cDNA synthesis (15). The cDNA was ligated into dephosphorylated, EcoRI digested lambda gt10 vector according to manufacturer's instructions (Stratagene, La Jolla, CA). The cDNA library was then packaged (Stratagene) using the Giga-pack 11 Gold Kit and amplified in C600hfl bacteria. Each library was amplified and plated onto 4 8 × 8 inch NUNC plates. Plaques on each plate were serially lifted onto 6 Hybond N membranes (17, 18). These membranes were then used for the screening of the libraries with the subtracted probe.

Subtractive Hybridization

Subtractive hybridization (19) was performed using nonbiotinylated cDNA inserts derived from the astrocytoma library and a 10-fold excess of biotinylated cDNA inserts from the glioblastoma library. cDNAs were polymerase chain reaction (PCR) amplified using lambda gt10 amplimers (Clontech, Palo Alto, CA) to enrich the subtraction with cDNA-specific sequences. PCR was performed using the Perkin-Elmer Geneamp 9600 system and the following program: 1 cycle of 94°C for 30 sec, 50°C for 15 sec, 72°C for 1 min, followed by 30 cycles of 94°C for 15 sec, 50°C for 15 sec, 72°C for 1 min and a final 7 min extension at 72°C. After PCR amplification, EcoRI restriction enzyme digestion and subsequent precipitation removed the amplimer sequences from the amplified cDNA sequences. The GBM cDNA was subjected to 2 rounds of biotinylation (20) using photoactivatable biotin (Clontech; super XX-PAB, cat. #5030-1). For the subtractive hybridization, 7.0 µg of biotinylated GBM cDNA was combined with 0.7 µg of nonbiotinylated astrocytoma cDNA. After 48 hours, the cDNA hybridization mix was applied to an iminodiacetic acid agarose column (Pierce Chemical, Rockford, IL) to which only the biotinylated cDNA remained attached (21). The flow-through was collected and reapplied to the column 3 times to ensure removal of biotinylated DNA. The final eluted nonbiotinylated subtracted astrocytoma cDNA was then purified us-

ing a Qiagen column according to manufacturer's instructions (Qiagen, Santa Clarita, CA). The subtracted cDNA was then rehybridized with 3.5 µg of freshly biotinylated GBM cDNA and the entire subtractive hybridization process was repeated. The subtracted cDNA was radiolabeled (see below) and used to screen the lifts of the astrocytoma cDNA library. Duplicate positive plaques were picked and processed through secondary and tertiary screens. Tertiary positive plaques were pulled and amplified after which the cDNA inserts were PCR amplified using lambda gt10 amplimers (Clontech). PCR products were purified from agarose gels using the Qiaex II Gel Extraction Kit, radiolabeled and hybridized to northern blots to verify differential expression (see below). A cDNA from tertiary screen plate #15 was subcloned into the TA Cloning vector (Invitrogen, Carlsbad, CA). Plasmid miniprep number 10 had the correct sized insert compared with the PCR product and consistently reproduced a differentially expressed signal on a variety of northern blots, and thus was designated "sc10."

Tissue Samples

Immediately upon surgical removal, tumor samples were fixed in 10% buffered formalin and embedded in paraffin for pathological diagnosis. These specimens were subsequently used for in situ hybridization and immunohistochemical analyses. The majority of the remaining tumor tissue was immediately snap-frozen in liquid nitrogen, while a small portion was disaggregated to start primary cell cultures. Glioma specimens were categorized by grade according to the World Health Organization grading system (22). Institutional IRB-approved informed consent was obtained from all patients or the patient's guardian.

Cell Lines

All cell lines are human derived. U251MGn and U251MGp are subclones of U251MG originally obtained from Põnten and MacIntyre (23) where "p" designates the original Põnten culture and "n" designates a subculture subsequently derived from U251MGp. U87MG was obtained from ATCC. Fetal astrocytes were purchased from Clonetics (San Diego, CA).

Northern Blots

Northern screening blots were prepared with RNA from tumor tissues, cell lines, and normal brain. Each clone was analyzed to 1) determine whether differential expression of the candidate gene was a result of the overexpression or underexpression in the tumor compared with normal brain, 2) determine the transcript size, 3) quantitate the level of differential expression, and 4) study the expression in tumor progression. RNA was extracted using the guanidium thiocyanate procedure (24) and quantitated by measuring absorbance at 260 nm. Samples were electrophoresed through a 1.2% formaldehyde-agarose gel in the presence of ethidium bromide and transferred to Hybond N (17). Following prehybridization, the filters were hybridized to a ³²P-dATP radiolabeled sc10 (SPARC) probe (radiolabeled using the Random Primer labeling kit [BRL] according to manufacturer's instructions), stringency washed and exposed to x-ray film. After probe stripping, the blots were similarly prehybridized and rehybridized to a glyceraldehyde phosphate dehydrogenase (GAPDH) probe. The 2.3 kb SPARC and the 1.4

kb GAPDH transcript abundances were determined by quantifying the hybridization signals on x-ray film using the NIH image densitometric software analysis as previously reported (25). The abundance of SPARC in each sample was corrected for loading variations by normalizing the values to the GAPDH signal for that lane. The percentage transcript abundance for each sample was expressed as a percentage of the maximum value for a given blot. The fold increase in tumor tissues was calculated as a fold increase above levels observed in normal brain tissues. Each blot shared samples, which were used to normalize results between blots. The mean value of the results from 3 northern blots is presented for normal specimens and tumors of each grade.

Western Blot Analysis

Intracellular SPARC was extracted from near confluent primary astrocytic tumor cells grown in DMEM + 10% fetal calf serum (FCS) that were rinsed 3 times with phosphate buffered saline (PBS) and then scraped and lysed with 2.5 ml of a single detergent lysis buffer (50 mM Tris HCl; pH 8.0, 150 mM NaCl, 0.02% sodium azide, 100 μ g/ml PMSF [phenylmethylsulfonyl fluoride], 1% Triton X-100) on ice. Lysed cells were centrifuged at 13,000 RPM in a microcentrifuge for 3 minutes at 4°C and the supernatants collected. SPARC secreted from tumor cells was collected from cells that were initially cultured in DMEM + 10% FCS medium, rinsed in PBS, and then cultured in Optimem serum-free medium for at least 7 days before medium collection to eliminate serum proteins for the western analyses. Protein concentration was determined using the BCA protein assay kit (Pierce Chemical). Approximately 15 μ g of total proteins, 5 μ l of protein molecular weight signals (BRL, Germantown, MD) and 5.8 ng of purified platelet-derived SPARC (Haematologic Technologies Inc., Essex Jct., VT) were mixed with an equal volume of 2X SDS reducing buffer (62.5 mM Tris-HCl; pH 6.8, 2% SDS, 5% 2-mercaptoethanol, 10% glycerol), boiled 3 min, and electrophoresed through a 10% polyacrylamide SDS Tris-glycine gel. Resolved proteins were transferred onto an Immobilon P membrane (Millipore, Bedford, MA). SPARC protein was detected using the chemiluminescence kit (Boehringer Mannheim Corp., Indianapolis, IN) after blocking in the supplied 1% blocking buffer for 1 hour, incubating with mouse anti-human osteonectin primary antibody (0.4 μ g/ml; Haematologic Technologies Inc.) for 1 hr, followed by incubating with secondary antimouse IgG-conjugated horseradish peroxidase antibody (1:1000 dilution; Sigma, St. Louis, MO) for 30 min, all at room temperature. The membrane was exposed to the primary detection reagent for 1 min and then exposed to film for 30 sec and developed.

Immunohistochemistry

Formalin-fixed, paraffin-embedded 5 μ m tissue sections were subjected to routine deparaffinization and rehydration. The subsequent steps were performed at room temperature unless otherwise specified. Sections were incubated for 10 min with 3% hydrogen peroxide in distilled water to inactivate endogenous peroxidases. Slides were then immersed in 10 mM sodium citrate buffer (pH 6.0) and boiled for 10 min on a hot plate and then allowed to cool for 20 min. Slides were rinsed in PBS solution and incubated with 1% bovine serum albumin in PBS

for 60 min to block nonspecific binding sites. The slides were then incubated overnight at 4°C with a 1:4800 dilution (0.74 μ g/ml) of primary anti-SPARC antibody (Haematologic Technologies Inc.) in PBS with 0.5% bovine serum albumin. After 3 washes in PBS buffer, the slides were incubated for 30 min with biotinylated secondary antibody (1:200 dilution in PBS), washed and incubated for 45 min with the avidin-biotin complex according to manufacturer's instructions (Vectastain ABC kit; Vector Laboratories, Burlingame, CA). Finally, the sections were washed, reacted with diaminobenzidine (DAB) in 0.1 M Tris buffer (pH 7.6) with 0.03% hydrogen peroxide, followed by rinsing in tap water, counterstaining, and mounting. Controls were performed omitting the primary anti-SPARC antibody. Slides were blindly reviewed and scored by a neuropathologist. Staining intensity was graded as negative (-), weak (+), moderate (++, +++), or strong (++++, +++++) for 0% staining, <20% of cells staining, 20–50% of cells staining, and >50% of cells staining, respectively.

Histomorphological Characterization of SPARC Expressing Cells

Cells were distinguished, in part, by their morphological features observed by hematoxylin and eosin-staining. Infiltrating neoplastic cells were identified as having large, pleomorphic, hyperchromatic, commonly elongated nuclei, with little or no detectable cytoplasm, i.e. naked nuclei (26). Reactive astrocytes were distinguished as cells with an appreciable amount of cytoplasm with star-like cytoplasmic processes and spatial symmetrical distribution (26).

Xenograft

Immunodeficient, RNU rats (Frederick Cancer Research and Developmental Center, Frederick, MD) were stereotactically injected with 5×10^6 U251MGp cells into the caudoputamen. The tumor was allowed to grow and invade for 4–6 weeks. The animals were perfusion fixed. The brains were immediately removed, further fixed and paraffin-embedded. Serial sections were obtained and every second section was subjected to in situ hybridization with a Blur-2 human-specific DNA probe (27) which would identify all human cells in the background of rat cells (see below). The alternate adjacent sections were subjected to immunohistochemical localization of SPARC protein as described previously.

Blur 2 DNA In Situ Hybridization

Formalin-fixed, paraffin-embedded 5 μ m tissue sections were cut and mounted on Superfrost/Plus precleaned slides (Fisher, Pittsburgh, PA). The following steps were performed at room temperature unless otherwise indicated. Fixed sections were rehydrated according to standard procedures, incubated in 200 mM HCl for 20 min, rinsed in distilled water, transferred to 2XSSC (300 mM NaCl, 30 mM Na₂C₂H₃O₂·2H₂O) for 30 min at 70°C, rinsed in distilled water, digested in 1 mg/ml proteinase K in 20 mM Tris-HCl; 2 mM CaCl₂, pH 7.4 for 1 min at 37°C, and washed twice for 5 min in distilled water. Sections were fixed in 5% paraformaldehyde for 1 hour followed by 2 rinses in 2XSSC. Sections were incubated in prehybridization buffer (5XSSC, 0.02% SDS, 50% formamide, 2% blocking reagent [Boehringer Mannheim kit], 0.5% N-lauroylsarcosine, 0.2 mg/

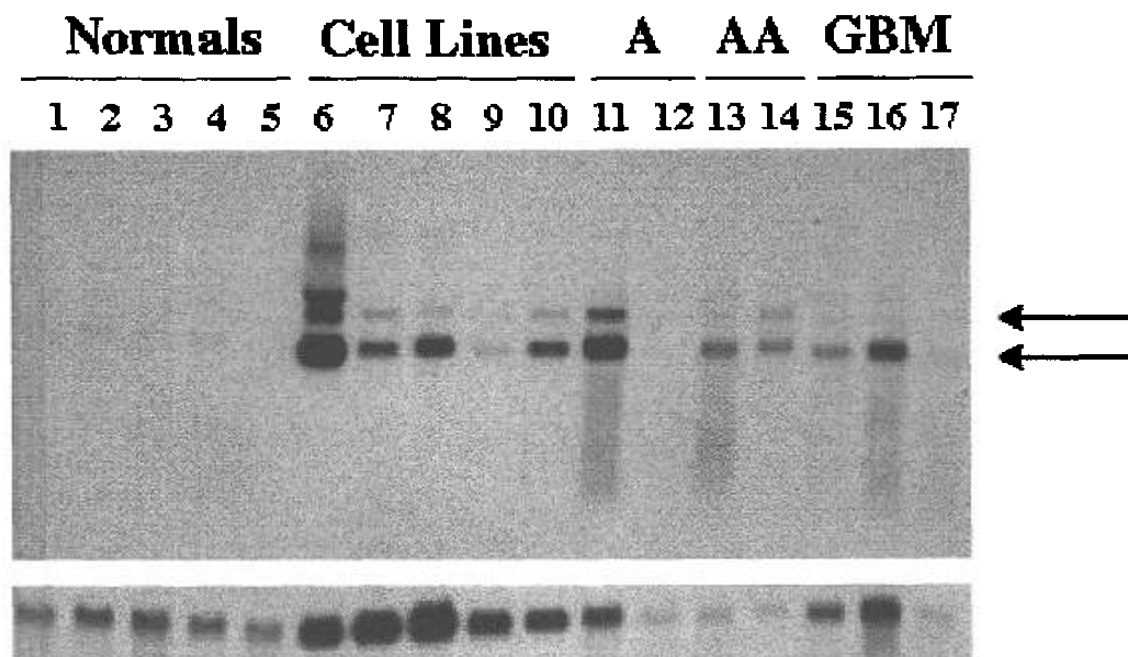


Fig. 1. Northern blot analysis of SPARC (sc10) mRNA in normal brain, established cell lines and tumor tissues. Total RNA (10 μ g/lane) extracted from normal brain, exponentially growing cells and tumor tissues was electrophoresed through 1.2% formaldehyde-agarose gel, transferred to a nylon membrane, hybridized to a 32 P-radiolabeled SPARC (sc10) cDNA probe, stripped, and rehybridized to a 32 P-radiolabeled GAPDH probe (17, 25). Top panel: SPARC probe hybridized to: Normals: normal brain (lanes: 1—HF178, 2—HF211, 3—HF232, 4—HF303, 5—HF312); Cell Lines: (lanes: 6—fetal astrocytes, 7—U251n, 8—U251p, 9—U87, 10—HF66); A: astrocytomas (lanes: 11—HF203, 12—HF250); AA: anaplastic astrocytomas (lanes: 13—HF34, 14—HF152) and GBM: glioblastomas (lanes: 15—HF138, 16—HF142, 17—HF218). The SPARC probe detected both the 3.0 kb (top arrow) and the 2.3 kb (bottom arrow) transcripts. Bottom panel: control GAPDH probe. (Note: the difference in mobility in the bands was introduced during electrophoresis and does not represent changes in the size of transcripts.)

ml sheared herring sperm DNA) in a humidity box for 30 min. After 2 washes in 2XSSC, sections were immersed in 70% formamide-2XSSC solution for 10 min at 70°C and then transferred to ice-cold distilled water. Sections were dehydrated through 70%, 95%, and 100% ethanol and air-dried prior to hybridization with the Blur 2 probe. The Blur 2 probe was labeled with the DIG-Chem-Link Labeling kit according to the manufacturer's instructions (28). Sections were hybridized with 5 ng/ml DIG-labeled probe in prehybridization buffer overnight. After hybridization, the sections were washed twice in 2XSSC for 5 min at room temperature and twice for 15 min at 55°C. Prior to detection, the sections were dipped briefly in washing buffer (0.1 M maleic acid, 0.15 M NaCl, 0.3% Tween-20) and then incubated in blocking solution (1% blocking reagent in 0.1 M maleic acid, 0.15 M NaCl) for 30 min at room temperature. Hybridized probe was detected using the DIG Nucleic Acid Detection Kit (Boehringer Mannheim) according to manufacturer's instructions using a 1:5000 dilution of anti-DIG-AP antibody for 1 hr. The color reaction was developed in BCIP-NBT solution overnight in the dark (approximately 20–24 hrs). After the reaction was terminated, sections were counterstained in 0.25% eosin-Y and the slides were mounted using an aqueous mounting medium (Paramount Aqueous Mounting Media, DAKO Corporation, Carpinteria, CA).

RESULTS

Subtractive hybridization was performed using nonbiotinylated cDNA inserts derived from the astrocytoma

library and a 10-fold excess of biotinylated cDNA inserts from the glioblastoma library. Subtraction resulted in the isolation of 58 clones, including the clone designated as sc10. Northern blot analysis indicated that sc10 expression was differentially expressed, i.e. low in normal brain RNA and upregulated in tumor RNA (Fig. 1).

Because the expression of the transcript was low in normal brain, multiple normal tissue poly A+ northern blots were used to determine whether a high abundance of transcript was detectable in another tissue. A 2.3 kb transcript detected by the sc10 probe was observed in all tissues examined with high levels of expression found in placenta (data not shown). To obtain the entire cDNA for sequence analysis, a 5' RACE-generated placenta cDNA (2.1 kb) was cloned into the pGEM-T vector. The 5' and 3'-generated cDNA sequence was submitted to Genebank and 100% homology was found to SPARC cDNA sequence (data not shown, 2).

The SPARC (sc10) cDNA hybridized to a major 2.3 kb transcript and a minor approximate 3.0 kb transcript which were differentially expressed between normal brain tissues and astrocytic tumors (Fig. 1; the transcripts are the same size in normal and tumor specimens and the apparent differences in motility were introduced during electrophoresis). The 2 transcripts are polyadenylation

TABLE 1
SPARC Transcript Abundance in Human Astrocytic
Tumors and Established Cell Lines

Tissue/cell lines	# of Specimens	Fold increase (2.3 kilobase transcript)
Normal	8	—
Astrocytoma	3	10.4 (1.5–15.0)
		HF202 15.0
		HF203 14.8
		HF250 1.5
Anaplastic astrocytoma	8	10.1 (0.5–17.1)
		HF26 11.6
		HF34 17.1
		HF152 16.9
		HF189 11.2
		HF191 0.5
		HF252 12.1
		HF298 5.9
		HF491 5.6*
Glioblastoma multiforme	9	3.6 (0.3–7.8)
		HF138 4.5
		HF140 0.4
		HF142 7.4
		HF212 0.9
		HF218 7.8
		HF274 3.8
		HF300 5.7
		HF350 2.0
		HF442 0.3*
Fetal astrocytes		22.6
U251MGn		7.4
U251MGp		9.6
U87		1.7
HF66		9.8

The fold increase in transcript abundance for the tissue samples presented in Fig. 1 and additional northern blots (not shown) is presented as the mean (range) followed by the average fold increase observed in individual tumors.

* Denotes samples with partial degradation leading to an underestimate of transcript abundance. These were included in the mean estimates as their omission did not significantly alter the results.

variants of the same gene (reviewed in 2). In addition, a larger transcript was observed in the human fetal astrocyte cell line. This transcript was not observed in any of the other normal adult tissues examined (data not shown) suggesting that it may be a developmentally regulated variant of the transcript. Densitometric analysis of the 2.3 kb transcript abundance was performed on 3 such northern blots (including that in Fig. 1) analyzing a total of 8 normal brain specimens, 3 astrocytomas (A), 8 anaplastic astrocytomas (AA), 9 GBMs, and 5 cell lines (Table 1). On average, an approximate 10-fold increase in SPARC transcript abundance was observed in astrocytoma and anaplastic astrocytomas (with an 11.2-fold increase in the anaplastic tumor HF189 when compared with levels in the normal brain tissue of the same patient). An approximate 4-fold increase was observed in glioblastomas

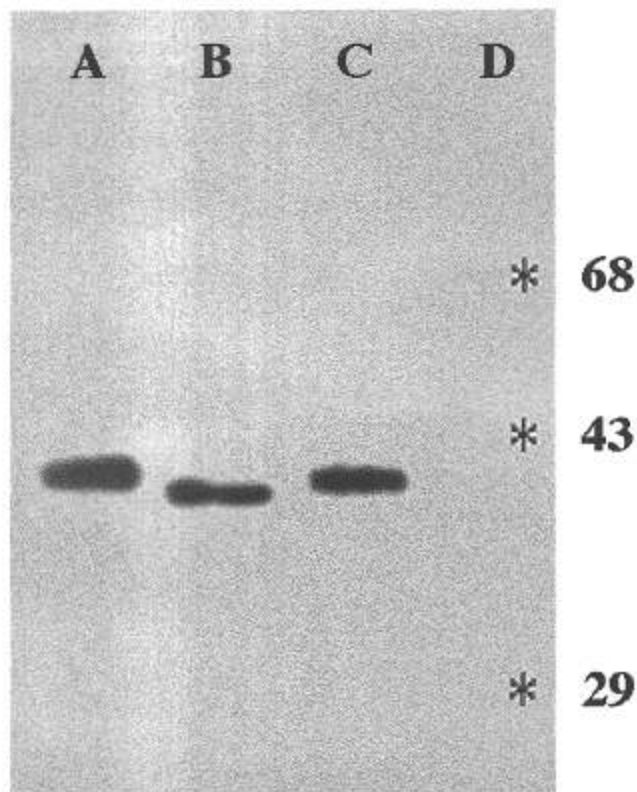


Fig. 2. Immunoblot of intracellular and secreted SPARC. The size of SPARC protein detected in 15 µg HF463 cell lysate (B) and 15 µg HF463 cell culture media (C) was compared with control, platelet-derived SPARC (A) and molecular weight standards (D). The electrophoretic mobility of secreted SPARC (C) is the same as that observed for the control with a Mr = 39,000 and migrates more slowly than the intracellular SPARC (B) with Mr = 36,000 due to differences in glycosylation (29).

when compared with levels detected in normal brain. The abundance was approximately 2.5-fold greater in lower grade tumors than in the GBMs. Human fetal astrocytes had the highest level of SPARC transcript abundance. We did not quantitate the 3.0 kb transcript that was variably expressed in tumors of all grades and absent in many samples examined.

To examine anti-SPARC antibody specificity and to characterize tumor SPARC protein, western blot analyses were performed on protein isolated from both tumor cell lysates and tumor cell conditioned media. The anti-SPARC antibody detected protein in both tumor cell lysates and in cell culture medium, as illustrated for sample HF463 (Fig. 2). In agreement with a previous report (29), we observed the size of the intracellular SPARC (Fig. 2B) to be smaller (Mr = 36,000) than that observed for the secreted SPARC (Fig. 2C; 12) which comigrates with the purified platelet-derived osteonectin control (molecular weight of 39,000; Fig. 2A). These results illustrate that the antibody is SPARC-specific and could be used to perform immunohistomorphological analyses.

TABLE 2
SPARC Protein Abundance in Human Astrocytic Tumors

Tissue/cell lines	# of Specimens	Tumor	Staining intensity	
			T.C.	E.C.
Normal	4		-	-
Astrocytoma	3	HF202	++	-
		HF203	+++	-
		HF250	++ to +++	++
Anaplastic astrocytoma	10	HF26	++	-
		HF34	-	++
		HF108	-	++
		HF110	++	-
		HF152	++++	- to ++++
		HF189	+++ to +++++	-
		HF191	++	++
		HF252	- to +++-	++
		HF298	++++	-
		HF491	++	-
Glioblastoma multiforme	9	HF50	- to ++++	++++ to +++++
		HF73	++++	-
		HF130	-	++
		HF138	++	++++
		HF140	++	++++
		HF142	-+	++++
		HF268	+++	-
		HF300	+++++	++++
		HF350	++++	++

Immunohistochemical staining intensity for the tissue samples in Fig. 2 and additional tumors (not shown) is presented as: negative (-), weak (+), moderate (++/+++), and strong (++++, +++++).

T.C. denotes tumor cells and E.C. denotes endothelial cells. If more than 1 paraffin-embedded section was available, the range of staining intensity was reported.

To characterize SPARC protein localization and expression levels during tumor progression, immunohistochemical analyses were performed on paraffin-embedded tissue sections of normal brain and tumors of all grades including 3 astrocytomas, 10 anaplastic astrocytomas, and 9 glioblastomas (Table 2). Elevated SPARC protein was observed in tumors of all grades (Fig. 3), in the cytoplasm of the tumor cells (Fig. 3B-I) and/or neovessel endothelial cells (Fig. 3F, H, I; Table 2). Variable levels of expression were observed between tumors of different grade, i.e. astrocytoma (Fig. 3B) and GBM (Fig. 3H, I), and between tumors within the same grade, i.e. anaplastic astrocytomas (Fig. 3D-E) and GBMs (Fig. 3G-I). In addition, variability in expression levels was also observed in tissue sections taken from different regions within the same tumor (Fig. 3E, F). (In situ hybridization with SPARC antisense and sense RNA probes was performed [data not shown] and demonstrated that transcript was present in both the astrocytic tumor cells and in neovessel endothelial cells, thus indicating that SPARC was independently synthesized in both cell types.)

To characterize SPARC expression in the context of regional tumor heterogeneity, we performed immunohistochemical analyses on specimens representing histologically diagnostic tumor, tumor/brain interface, and adja-

cent normal brain, which were removed from a glioblastoma patient (HF50) with the use of an intraoperative stereotactic imaging wand (Fig. 4). Within the region of diagnostic tumor we observed densely cellular regions containing undifferentiated cells with high nucleocytoplasmic ratio (highly characteristic of high grade gliomas) with adjacent less cellular regions composed of better differentiated cells of astrocytic phenotype with variably abundant cytoplasm. Elevated SPARC expression was commonly observed in a subpopulation of tumor cells in the less cellular regions (Fig. 4A). In the brain immediately adjacent to the tumor at the tumor/brain interface, SPARC expression was greatly elevated in the neoplastic-appearing cells, in reactive astrocytes, and in the endothelial cells of neovessels (Fig. 4B). In the specimen representing adjacent normal brain, highly elevated SPARC expression was observed in individual cells, presumably a combination of invading tumor cells and reactive astrocytes (Fig. 4C). The same observations were made on other tumor specimens that also had adjacent brain tissue available for examination.

To confirm that SPARC expression was enhanced in invading tumor cells, adjacent paraffin-embedded sections of a human U251MGp xenograft tumor in rat brain were analyzed either by in situ hybridization with the

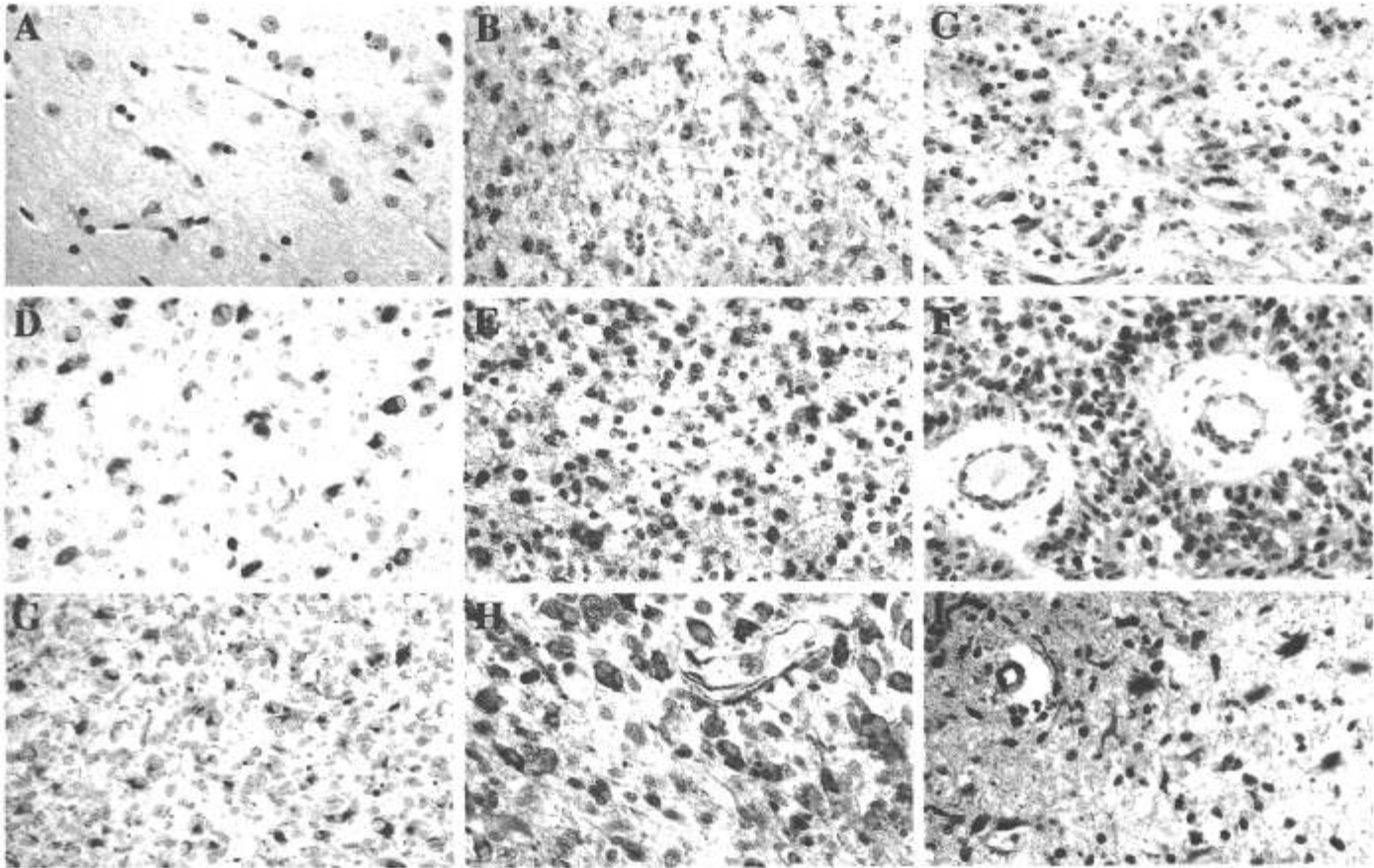


Fig. 3. Immunohistochemical localization of SPARC protein in normal brain and tumor tissues. SPARC protein was localized in normal brain, astrocytoma (A), anaplastic astrocytoma (AA), and glioblastoma (GBM) tissue sections using a 1:4800 dilution of anti-SPARC (osteonectin) antibody and detection with a diaminobenzidine reaction as described in Materials and Methods. All magnifications are $\times 40$. A. Normal cerebral cortex (HF252), B. A (HF250), C. A (HF631), D. AA (HF491), E. AA (HF152, nonvascular region), F. AA (HF152, abnormal vessels), G. GBM (HF268), H. GBM (HF350), I. GBM (HF300). A positive reaction is observed in all tumors. There are variable levels of expression in different regions of the same tumor, in tumors within the same grade, and in tumors of different grades. The positive cytoplasmic reaction is present in both tumor cells and neovessel endothelial cells. The cytoplasmic localization of SPARC is also observed in Figure 4.

Blur 2 human-specific ALU repeat DNA probe (Fig. 5A, B; Fig. 6A, B) or, immunohistochemically with anti-SPARC antibody (Fig. 5C, D; Fig. 6C, D). The results demonstrated colocalization of the Blur 2 DNA probe and the SPARC immunohistochemical signals to human cells of the tumor mass and to human tumor cells invading adjacent rat brain, including human tumor cells surrounding vascular structures and individual tumor cells in the brain parenchyma.

DISCUSSION

To identify genetic alterations occurring early in astrocytoma progression, we performed subtractive hybridization between astrocytoma and glioblastoma cDNA libraries. Using this technique, we have identified SPARC, a developmentally regulated gene implicated in the modulation of cell-matrix interactions, as a gene that is inappropriately overexpressed early in astrocytic tumor

progression (in agreement with a previous observation [11]) and in astrocytic tumors of all grades.

SPARC's expression profile was found to be complex and dictated by the extent of tumor heterogeneity. Densitometric northern blot analysis (Fig. 1) indicated that SPARC expression was greater in the lower grade tumors (astrocytomas and anaplastic astrocytomas) than in the GBMs (Table 1), the expression profile targeted by the subtraction procedure. However, variable levels of expression were observed between tumors within a given grade. The cause of the variability in the transcript abundance was explained by the immunohistochemical analyses (Fig. 3; Table 2) and confirmed by *in situ* hybridization using antisense and sense control SPARC RNA probes (data not shown). SPARC protein (Fig. 3) and transcript (data not shown) were observed in both the astrocytic tumor cells and in the neovessel endothelial cells. The expression was, therefore, not cell-type specific

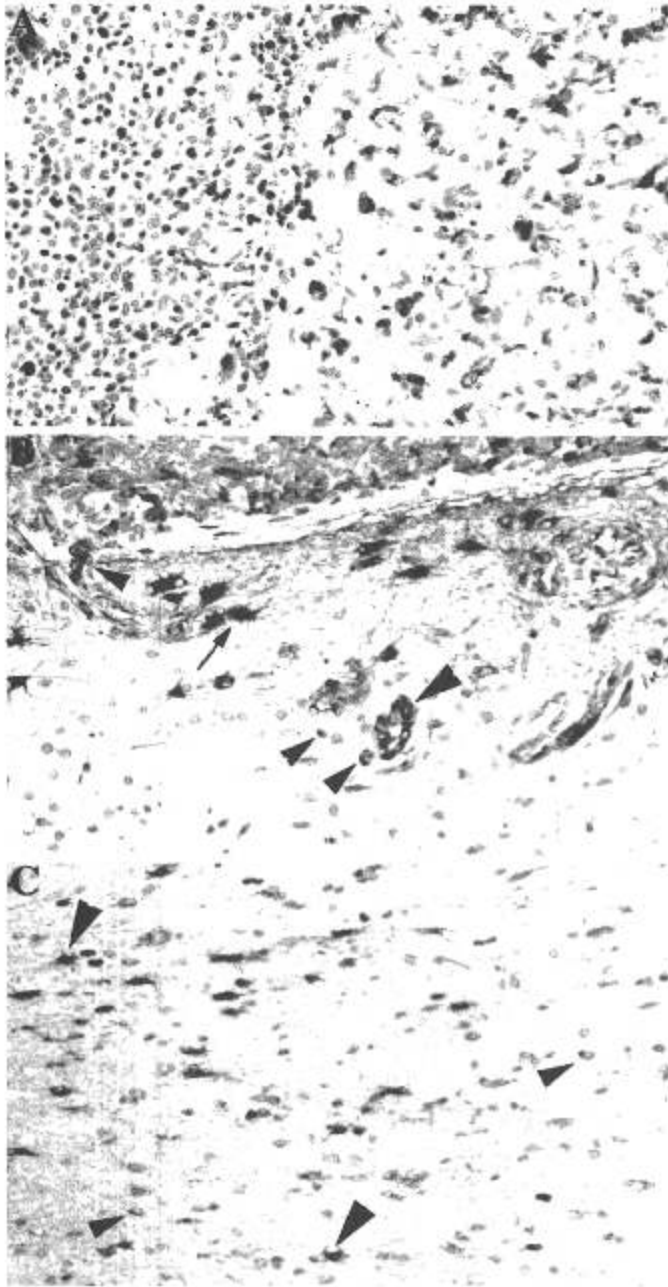


Fig. 4. Heterogeneous SPARC Expression. SPARC protein was immunohistochemically localized as described in Figure 3. Three stereotactically removed specimens of HF50 tumor and adjacent brain tissues are illustrated ($\times 20$). A strong positive cytoplasmic reaction is observed in a subpopulation of better-differentiated cells in the region of histologically diagnostic tumor (A), in infiltrating tumor cells (B, small arrowheads), reactive astrocytes (B, arrow) and endothelial cells of neofomed vessels (B, large arrowhead) in the brain at the tumor/brain interface (B), and in individual cells appearing to be a mixture of tumor cells (small arrowheads) and reactive astrocytes (large arrowheads) in the adjacent normal brain (C).

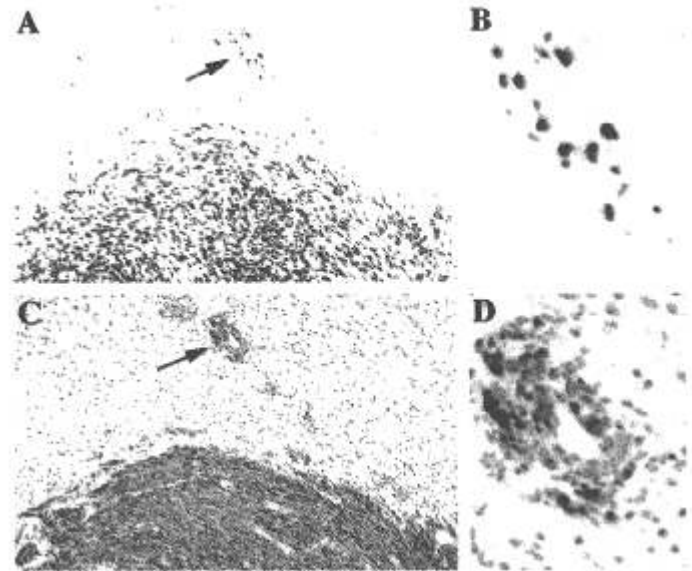


Fig. 5. SPARC Expression in Tumor Cells Invading Along Vascular Basement Membranes in Human/Rat Xenograft. A and B: In situ hybridization with the human specific DNA-detecting Blur 2 probe. A, $\times 20$ and B, approximately $\times 40$. Vessel in A (arrow) is magnified in B. C and D: SPARC immunohistochemical localization. C, $\times 20$ and D, approximately $\times 40$. The positive Blur 2 reaction in perivascular cells indicates the presence of infiltrating human tumor cells. The SPARC stain demonstrates that these infiltrating tumor cells possess a high level of the protein. (Note: the staining patterns are not identical because the Blur 2 probe hybridizes to DNA in the nucleus and the antibody binds to SPARC in the cytoplasm.)

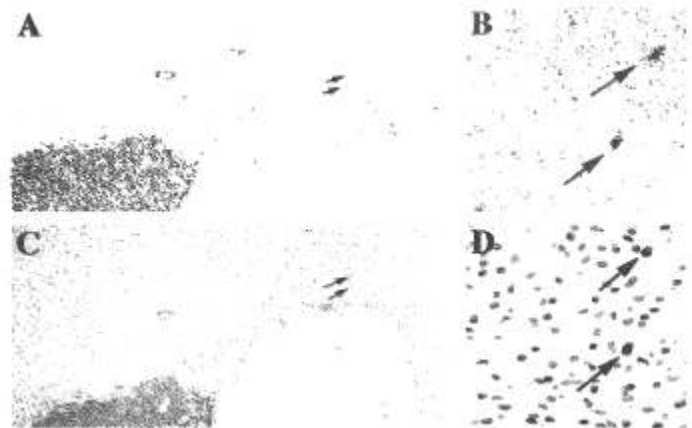


Fig. 6. SPARC expression in Tumor Cells Invading into Brain Parenchyma. A and B: In situ hybridization with the human-specific DNA-detecting Blur 2 probe. A, $\times 20$ and B, approximately $\times 40$. Cells in A (arrows) are magnified in B (arrows). C and D: SPARC immunohistochemical localization. C, $\times 20$ and D, approximately $\times 40$. Cells in C (arrows) are magnified in D (arrows). The positive Blur 2 reaction is observed in individual human tumor cells invading into rat brain parenchyma. The SPARC signal colocalizes with the human DNA signal, demonstrating SPARC expression in human tumor cells that have migrated a great distance away from the tumor mass seen in A and C.

and consequently the northern blot analyses represent a compound signal derived from tumor and endothelial cells.

In addition, regional differences in the SPARC protein levels were correlated with tumor heterogeneity using individual specimens taken from within the same tumor. In heterogeneous GBM tumor tissue, high SPARC expression was associated with the less cellularly dense regions of the tumor composed of better differentiated tumor cells (Fig. 4). Thus, a tumor with extensive areas of better differentiated tissue with prominent neovascularization may actually have more SPARC than a tumor with a more homogeneous population of less differentiated cells with sparse neovascularization. A large low grade tumor could conceivably have more SPARC than a high grade tumor. Therefore, the extent of both tumor heterogeneity and neovascularization, combined with regional sampling differences, appears to dictate the overall level of SPARC expression in a tumor-dependent rather than grade-related manner.

When taking SPARC function into account, these observations suggest that SPARC may be an astrocytoma candidate invasion-related gene. It has been reported that SPARC binds directly to vitronectin and the balance of expression of these 2 proteins can modulate cell adhesion to ECM. Vitronectin is a constituent of brain vascular basement membranes, 1 of the preferred routes taken by astrocytomas. Furthermore, SPARC interactions with the collagens may play a role in the single cell invasion into brain parenchyma. Thus, increased SPARC expression may confer a more migratory/invasive phenotype to the astrocytomas.

To further establish the correlation between SPARC expression and invading tumor cells, we used the human/rat xenograft which recapitulates the different clinical patterns of glioma infiltration/invasion including single cell infiltration of adjacent parenchyma, the invasion of cells along perivascular basement membrane, and the movement of cells along white matter pathways (reviewed in 30). SPARC-positive human tumor cells were observed invading adjacent brain along endogenous rat vessels (Fig. 5) and as individual human tumor cells invading at a great distance into the brain parenchyma (Fig. 6). These data demonstrate that invading tumor cells overexpress SPARC protein, supporting the hypothesis that it may functionally contribute to tumor cell migration/invasion.

Increased SPARC expression has been associated with repair processes such as wound healing (5) and as such may be considered a stress response gene. When the brain is injured, astrocytes in the region of stress may become activated. We observed increased SPARC expression in reactive astrocytes in brain tissue adjacent to the tumor (Fig. 4). Reactive astrocytes and neoplastic cells often share histomorphological features, making them difficult

to distinguish from one another. Furthermore, there are no specific markers to aid in this dilemma. However, the SPARC-positive, highly swollen and hypertrophic reactive astrocytes appear to be distinguishable from the SPARC-positive tumor cells by the combination of both their morphology (26; Fig. 4) and the GFAP-staining pattern (data not shown). Thus, enhanced SPARC expression in these hypertrophic reactive astrocytes may be indicative of the regional extent of tumor-associated stress in the adjacent brain tissue. Interestingly, reactive astrocytes secrete fibronectin (31), an ECM molecule that supports migration of glial tumor cells along blood vessels (32). Thus, the response of the reactive astrocytes in the adjacent brain may, ironically, indirectly contribute to tumor cell invasion into adjacent brain parenchyma (33).

If SPARC directly contributes to invasion, the western blot analyses (Fig. 2) suggest that the SPARC protein isolated from the tumor cells appears to be normally glycosylated and secreted. In addition, our southern blot analysis (data not shown) indicates no gross structural abnormality in the gene. Thus, the inappropriate timing of increased expression of a developmentally regulated gene may contribute to the invasive phenotype. Our ongoing experiments are pursuing this hypothesis.

In summary, we have identified SPARC as a gene overexpressed in astrocytic tumors of all grades. In addition to expression in neovessel endothelial cells, SPARC is highly expressed in cells within the tumor mass, in tumor cells invading adjacent brain, and in reactive astrocytes at the brain tumor interface. These data suggest that SPARC overexpression occurs early in astrocytoma progression, is a candidate invasion-related gene, and may serve as a signal of both neoplastic astrocytic transformation and reactive response to tumor presence.

ACKNOWLEDGMENTS

We thank Dr. Mark L. Rosenblum for support of these studies, Dr. Oliver Bögler and Dr. Irene Newsham for critical reading of the manuscript, Dr. Web Cavenee for use of the libraries, Dr. Carl Schmidt for the Blur 2 probe, Dr. Xiao Yi Yang for preparation of paraffin-embedded xenograft sections, Nicole Miller for northern blot preparations, and our neurosurgeon colleagues for the appropriate collection of tumor specimens.

REFERENCES

1. Rempel SA. Molecular biology of central nervous system tumors. *Curr Opin Oncol* 1998;10:179-85
2. Swaroop A, Hogan BLM, Franke U. Molecular analysis of the cDNA for human SPARC/osteonectin/BM-40: Sequence, expression, and localization of the gene to chromosome 5q31-q33. *Genomics* 1988;2:37-47
3. Sage EH. Terms of attachment: SPARC and tumorigenicity. *Nature Med* 1997;3:144-46
4. Mundlos S, Schwahn B, Reichert T, Zabel B. Distribution of osteonectin mRNA and protein during human embryonic and fetal development. *J Histochem Cytochem* 1992;40:283-91

5. Reed MJ, Puolakkainen P, Lane TF, Dickerson D, Bornstein P, Sage EH. Differential expression of SPARC and thrombospondin 1 in wound repair: immunolocalization and *in situ* hybridization. *J Histochem & Cytochem* 1993;41:1467-77
6. Mendis DB, Malaval L, Brown IR. SPARC, an extracellular matrix glycoprotein containing the follistatin module, is expressed by astrocytes in synaptic enriched regions of the adult brain. *Brain Res* 1995;676:69-79
7. Giese A, Loo MA, Rief MD, Tran N, Berens ME. Substrates for astrocytoma invasion. *Neurosurgery* 1995; 37:294-302
8. Rosenblatt S, Bassuk JA, Alpers CE, Sage EH, Timpl R, Preissner KT. Differential modulation of cell adhesion by interaction between adhesive and counter-adhesive proteins: Characterization of the binding of vitronectin to osteonectin (BM40, SPARC). *Biochem J* 1997;324:311-19
9. Murphy-Ullrich JE, Lane TF, Pallero MA, Sage EH. SPARC mediates focal adhesion disassembly in endothelial cells through a follistatin-like region and the Ca⁺⁺-binding EF-hand. *J Cellular Biochemistry* 1995;57:341-50
10. Tremble PM, Lane TF, Sage EH, Werb Z. SPARC, a secreted protein associated with morphogenesis and tissue remodeling, induces expression of metalloproteinases in fibroblasts through a novel extracellular matrix-dependent pathway. *J Cell Biol* 1993;121:1433-44
11. Porter PL, Sage EH, Lane TF, Funk SE, Gown AM. Distribution of SPARC in normal and neoplastic tissue. *J Histochem Cytochem* 1995;43:791-800
12. Bellacene A, Castronovo V. Increased expression of osteonectin and osteopontin, two bone matrix proteins, in human breast cancer. *Am J Pathol* 1995;146: 95-100
13. Porte H, Chastre E, Prevot S, et al. Neoplastic progression of human colorectal cancer is associated with overexpression of the stromelysin-3 and BM-40/SPARC genes. *Int J Cancer* 1995;64:70-75
14. Ledda M F, Adris S, Bravo AI, et al. Suppression of SPARC expression by antisense RNA abrogates the tumorigenicity of human melanoma cells. *Nature Med* 1997;3:171-76
15. Gubler U, Hoffman BJ. A simple and very efficient method for generating cDNA libraries. *Gene* 1983;25:263-89
16. Auffray C, Rougeon F. Purification of mouse immunoglobulin heavy-chain messenger RNAs from total myeloma tumor RNA. *Eur J Biochem* 1980;107:303-14
17. Maniatis T, Fritsch EF, Sambrook J. *Molecular cloning; a laboratory manual*. Cold Spring Harbor, NY: Cold Spring Harbor Press, 1989
18. Ausubel F M, Brent R, Kingston R E, et al. *Current Protocols in Molecular Biology*. New York: John Wiley and Sons, 1996
19. Schweinfest CW, Henderson KW, Gu J-R, et al. Subtraction hybridization cDNA libraries from colon carcinoma and hepatic cancer. *Genet Anal Techn Appl* 1990;7:64-70
20. Sive HL, St. John T. A simple subtractive hybridization technique employing photoactivatable biotin and phenol extraction. *Nucleic Acids Res* 1988;16:10937
21. Welcher AA, Torres AR, Ward DC. Selective enrichment of specific DNA, cDNA, and RNA sequences using biotinylated probes, avidin and copper-chelate agarose. *Nucleic Acids Res* 1986;14:10027-44
22. Kleihues P, Burger PC, Scheithauer BW. The new WHO classification of brain tumors. *J Brain Pathol* 1993;3:255-68
23. Pönten J, MacIntyre EH. Long term culture of normal and neoplastic human glia. *Acta Pathol Scand* 1968;74:465-86
24. Chomeczynski P, Sacchi N. Single-step method of RNA isolation by acid guanidium thiocyanate-phenol-chloroform extraction. *Anal Biochem* 1987;162:156-59
25. Rempel SA, Rosenblum ML, Mikkelsen T, et al. Cathepsin B expression and localization in glioma progression and invasion. *Cancer Res* 1994;54:6027-31
26. Dumas-Duport C, Scheithauer BW. A histologic and cytologic method for the spatial definition of gliomas. *Mayo Clin Proceed* 1987;62:435-49
27. Deininger PL, Jolly DJ, Rubin CM, Friedmann T, Schmid CW. Base sequence studies of 300 nucleotide renatured repeated human DNA clones. *J Mol Biol* 1981;151:17-33
28. Boehringer Mannheim GmbH. *Biochemica. Nonradioactive In Situ Hybridization Application Manual*, 2nd ed., 1996
29. Kelm RJ Jr, Hair GA, Mann KG, Grant BW. Characterization of human osteoblast and megakaryocyte-derived osteonectin (SPARC). *Blood* 1992;80:3112-19
30. Mikkelsen T, Edvardsen K. Tumor Invasiveness. In: Black P McL, Loeffler JS, eds. *Cancer of the nervous system*. Cambridge: Blackwell Science, 1997; 843-57
31. Pedersen P-H, Marienhagen K, Mork S, Bjerkvig R. Migratory pattern of fetal rat brain cells and human glioma cells in the adult brain. *Cancer Res* 1993;53:5158-65
32. McComb RD, Bigner DD. Immunolocalization of monoclonal antibody-defined extracellular matrix antigens in human brain tumors. *J Neurooncol* 1985;3:181-86
33. Friedlander DR, Zagzag D, Shiff B, et al. Migration of brain tumor cells on extracellular matrix proteins *in vitro* correlates with tumor type and grade and involves α v and β 1 integrins. *Cancer Res* 1996; 56:1939-47

Received March 31, 1998

Revision received June 23, 1998 and August 12, 1998

Accepted August 12, 1998